

## Theory of surface polaritons in germanium\*

B. G. Martin and R. F. Wallis

Department of Physics, University of California, Irvine, Irvine, California 92664

(Received 7 July 1975)

A theoretical investigation has been made of surface polaritons in germanium using experimental values of the complex dielectric constant. The surface-polariton dispersion curve and attenuation length were obtained from these data. In the higher-frequency region, the dispersion curve exhibits backbending. Zenneck modes were found in the small-wave-vector region (i.e., where  $k < \omega/c$ ). The use of attenuated total reflection for observing the surface polaritons in Ge is discussed.

### I. INTRODUCTION

Polaritons<sup>1</sup> are coupled modes of photons and elementary excitations such as phonons, plasmons, magnons, and excitons. Surface polaritons are polaritons which are associated with a semi-infinite dielectric medium where the coupled excitation is localized near the surface. In the absence of damping, surface-polariton modes occur in the region where the wave-vector magnitude  $k$  and frequency  $\omega$  satisfy the relation  $k > \omega/c$ , that is, the modes are nonradiative. A consequence of this nonradiative nature is that simple optical absorption cannot be used to investigate surface polaritons; however, the experimental technique of attenuated total reflection (ATR)<sup>2,3</sup> can be used. In the presence of damping, surface polaritons can exist in the region where  $k < \omega/c$ . Under these circumstances, they are known as Zenneck modes.<sup>4</sup>

We consider here the surface-polariton dispersion for a dielectrically isotropic crystal, namely, germanium. Experimental values of the complex dielectric constant were used in the calculations. A digital computer was used to calculate the real and imaginary parts of the wave vector associated with surface polaritons of frequency  $\omega$ , and other parameters of interest, e.g., the depth of penetration of the electric field.

Finally, some ATR calculations were made using the experimental values of  $\epsilon(\omega)$ . The ATR reflectivity vs angle of incidence was calculated for several photon energies. A comparison is made of the surface-polariton dispersion results and the ATR calculations.

### II. SURFACE-POLARITON DISPERSION CURVES

Using classical electromagnetic theory one can obtain the relation between the wave vector  $k$  and the frequency  $\omega$ , i. e., the dispersion relation, for surface polaritons. This dispersion relation can be written in the form<sup>5</sup>

$$k^2 = \frac{\omega^2}{c^2} \frac{\epsilon(\omega)}{1 + \epsilon(\omega)}, \tag{1}$$

where  $\epsilon(\omega) = \epsilon_1 + i\epsilon_2$ . In view of the complex nature of  $\epsilon(\omega)$ , we must take either  $k$  or  $\omega$  complex. We choose  $k$  to be complex and  $\omega$  to be real. Equation (1) follows from an alternative form

$$\epsilon(\omega) = -\alpha/\alpha_0, \tag{2}$$

where

$$\alpha^2 = k^2 - (\omega^2/c^2)\epsilon(\omega), \tag{3a}$$

$$\alpha_0^2 = k^2 - \omega^2/c^2 \tag{3b}$$

with  $\alpha$  being associated with the crystal and  $\alpha_0$  being associated with the vacuum. The quantities  $\alpha$  and  $\alpha_0$  are the decay coefficients of the electric vector in the direction normal to the surface. For a true surface wave, the real parts of  $\alpha$  and  $\alpha_0$  should be positive.

If one considers the case where no damping is present (i. e.,  $\epsilon_2 = 0$ ), the dispersion relation is, from Eq. (1),

$$k^2 = \frac{\omega^2}{c^2} \frac{\epsilon_1(\omega)}{1 + \epsilon_1(\omega)}. \tag{4}$$

Since this equation involves only real quantities, the surface polaritons which result have both  $\omega$  and

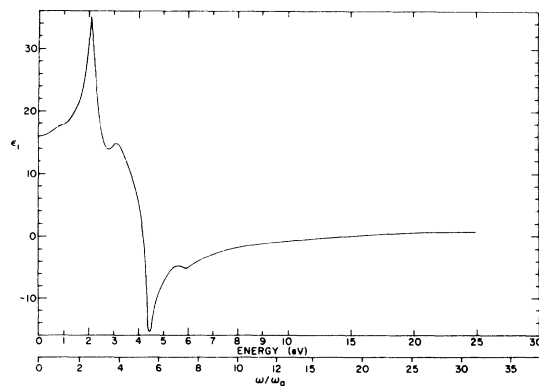


FIG. 1. Experimental results for the frequency dependence of the real part of the dielectric constant of germanium.

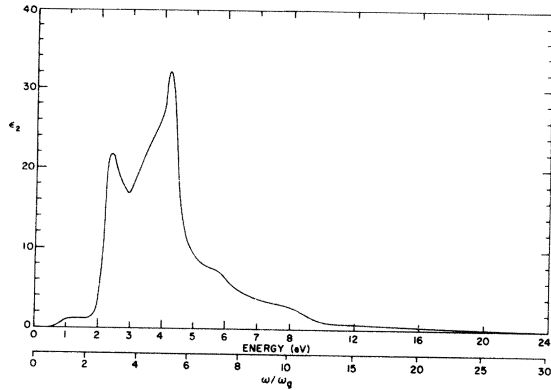


FIG. 2. Experimental results for the frequency dependence of the imaginary part of the dielectric constant of germanium.

$k$  real.

Some results for the complex dielectric constant of Ge are shown<sup>6</sup> in Figs. 1 and 2. These curves represent a Kramers-Krönig analysis of experimental reflectivity data obtained by Donovan, Ashley, and Bennett<sup>7</sup> and experimental data of Marton and Toots.<sup>8</sup> We can now obtain the dispersion curves for surface polaritons. A digital computer was used to calculate values for plotting the dispersion curves. The computer inputs are

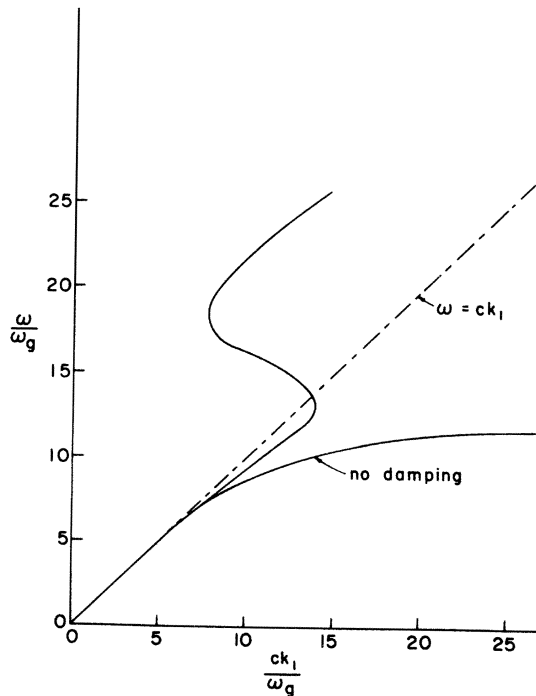


FIG. 3. Surface-polariton dispersion in germanium obtained by using experimental values of the complex dielectric constant.

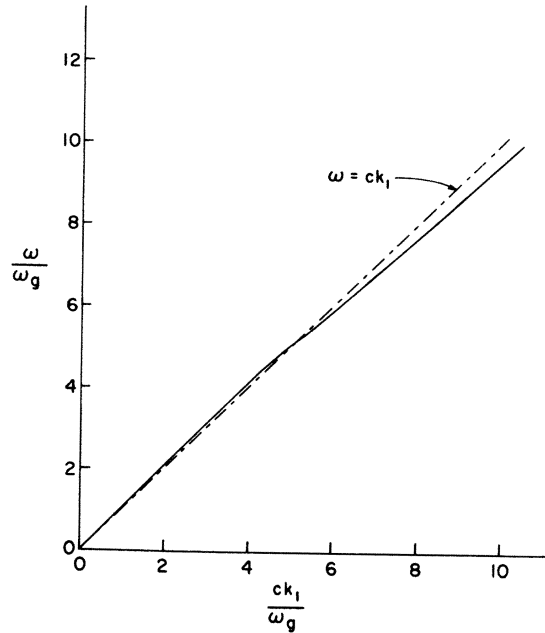


FIG. 4. Crossover point of surface-polariton dispersion in germanium.

$\epsilon_1$  and  $\epsilon_2$ . The outputs are  $ck_1/\omega_g$ ,  $ck_2/\omega_g$ ,  $c\alpha_1/\omega_g$ ,  $c\alpha_2/\omega_g$ ,  $c\alpha_{01}/\omega_g$ , and  $c\alpha_{02}/\omega_g$  where

$$\begin{aligned} k &= k_1 + ik_2, \\ \alpha &= \alpha_1 + i\alpha_2, \\ \alpha_0 &= \alpha_{01} + i\alpha_{02}, \end{aligned} \quad (5)$$

and  $\omega_g$  is the frequency associated with the gap (for Ge,  $\omega_g = 1.22 \times 10^{15}$  sec<sup>-1</sup>).

In Fig. 3 we present the surface-polariton dispersion curve; the curve shows backbending for  $\omega \geq 12\omega_g$ . This type of behavior has also been observed in silver.<sup>9</sup> We note from Fig. 3 that the dispersion curve crosses over to the left of the light line in the vicinity of  $\omega \approx 13.5\omega_g$ . Although it is not evident in this figure, the curve also lies to the left of the light line for  $\omega \leq 5.2\omega_g$ . Figure 4 shows the crossover point in more detail. In these regions, where the dispersion curve is to the left of the light line,  $\epsilon_1(\omega) < -1$  and we have Zenneck modes.

The imaginary part of the wave vector ( $k_2$ ) is plotted as a function of frequency in Fig. 5. The attenuation length  $L$  of the surface polariton can be obtained from  $k_2$  using the relation

$$L = 1/2k_2. \quad (6)$$

The values of  $L$  range from  $10^{-4}$  cm at  $\omega \approx 5\omega_g$  to  $10^{-6}$  cm at  $\omega \approx 15\omega_g$  to  $10^{-5}$  cm at  $\omega \approx 25\omega_g$ . We see that the attenuation length is quite short. The values of  $c\alpha_1/\omega_g$  range from  $\sim 0.2$  at  $\omega \sim \omega_g$  to  $\sim 19$  at  $\omega \sim 10\omega_g$ .

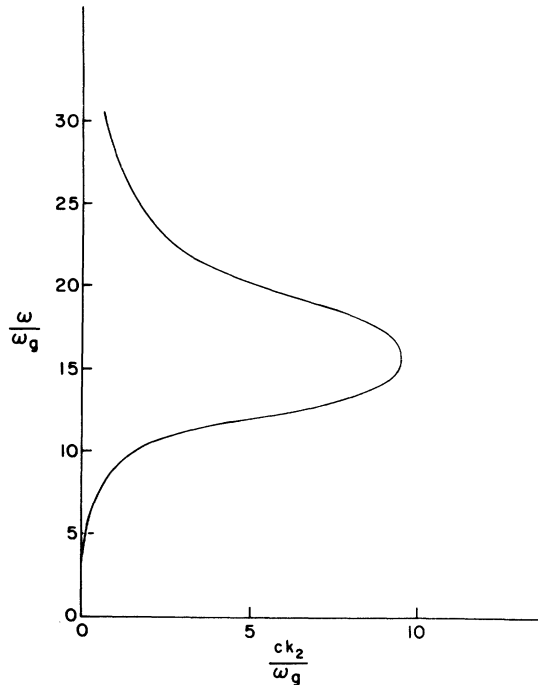


FIG. 5. Frequency dependence of the imaginary part of the wave vector associated with surface polaritons in germanium.

### III. ATR CALCULATIONS

Surface polaritons can be investigated experimentally by the attenuated total reflection (ATR) technique.<sup>2</sup> A prism is used to couple electromagnetic waves across a gap to a crystal surface. The result is a reflected wave whose intensity is a minimum if the frequency and wave vector are matched to the dispersion relation of a surface polariton propagating along the crystal surface. At the minimum reflectivity, a point on the dispersion curve can be obtained from the equation<sup>2</sup>

$$k = n_p(\omega/c)\sin\alpha, \quad (7)$$

where  $n_p$  is the refractive index of the prism at its transmission peak and  $\gamma$  is the angle of incidence of the beam. In ATR, the range of available  $k$  values is

$$\omega/c < k < n_p\omega/c \quad (8)$$

and the range for the angle of incidence is

$$\frac{1}{2}\pi \geq \alpha \geq \sin^{-1}(1/n_p) \quad (9)$$

if we assume an air gap.

In what follows, we present the results of ATR calculations where a  $\text{CaF}_2$  prism ( $n_p = 1.434$ ) is used. In addition, the use of a  $\text{LiF}$  prism ( $n_p = 1.938$ ) is discussed. The useful transmission range for  $\text{CaF}_2$  is from  $0.123$ ,<sup>10</sup> to  $9 \mu\text{m}$  which corresponds to a maximum frequency of

$\omega = 12.5\omega_g$ . For larger values of  $\omega$  (where back-bending in the surface polariton dispersion curve for Ge occurs), the  $\text{CaF}_2$  prism is not useful. However, a  $\text{LiF}$  prism with an approximate cutoff wavelength of<sup>11</sup>  $0.105 \mu\text{m}$  would transmit frequencies up to  $14.7\omega_g$ . Lithium fluoride is transparent to shorter ultraviolet wavelengths than any other available crystalline material.

The equation for reflectivity as a function of frequency, wave vector, and the real and imaginary parts of the complex dielectric constant is obtained from Fresnel's equations for both the TM and TE modes. Since we are considering surface waves, the equation for the TM mode is required. In what follows, the experimental values of the complex dielectric constant were used. Figure 6 shows the ATR reflectivity vs angle of incidence for several energies where the gap distance  $d$  between the  $\text{CaF}_2$  prism and the Ge crystal is  $0.025 \mu\text{m}$ . Figure 7 shows some results for  $d = 0.05 \mu\text{m}$ . From each minimum, a point on the surface-polariton dispersion curve was obtained using Eq. (7). From the figures, note that at higher frequencies, the ATR reflectivity curves become wider, indicative of higher damping at higher frequencies. A comparison of the ATR results and those we obtained before are given in Table I and show reasonable agreement, especially for  $d = 0.05 \mu\text{m}$ . To the authors's knowledge, no ATR experimental results are available for Ge so no comparison to the calculated values can be made.

In this paper, the wave vector  $k$  has been con-

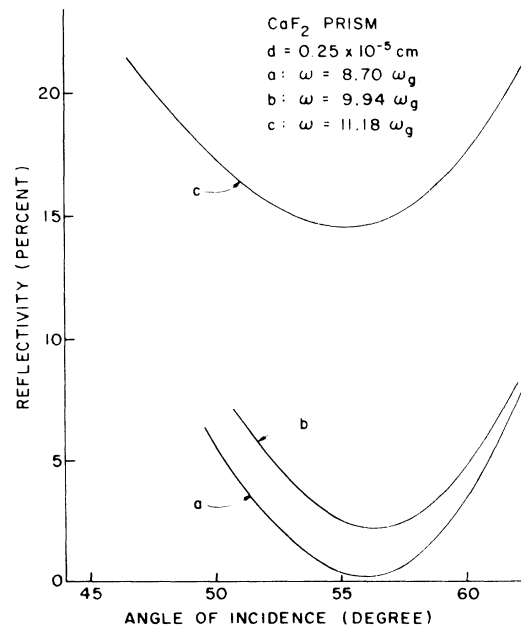


FIG. 6. ATR reflectivity vs angle of incidence for several incident energies: gap distance  $d = 0.025 \mu\text{m}$ .

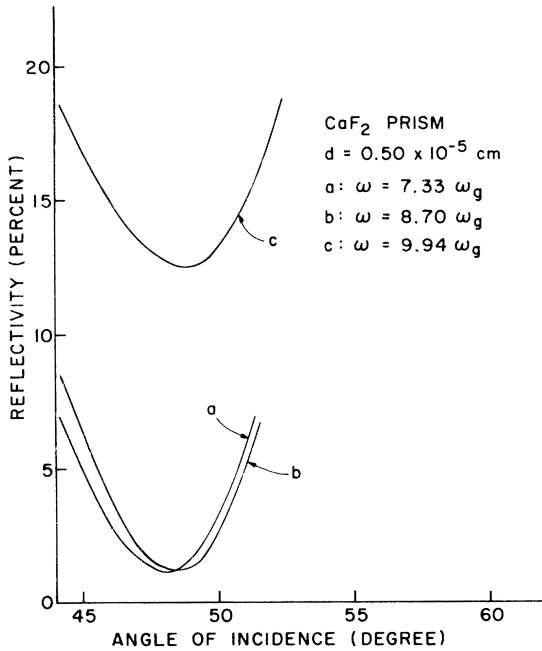


FIG. 7. ATR reflectivity vs angle of incidence for several incident energies: gap distance  $d=0.050 \mu\text{m}$ .

sidered as a complex quantity and  $\omega$  as a real quantity. ATR calculations can also be made where  $\omega$  is taken to be complex and  $k$  is taken as real. In the former case, one measures a finite decay length while in the latter, one measures a finite lifetime of the surface polaritons. In the ATR calculations reported here, where the angle  $\alpha$  is varied, the width of the dip in reflectivity is a measure of the imaginary part of  $k$ .

As discussed by Otto<sup>2</sup> and by Bishop,<sup>12</sup> the ratio of TE and TM modes assures that the dip in the ATR reflectivity curve corresponds to surface polaritons alone. Since we have done calculations only for the TM mode, a discussion of the behavior of bulk polariton dispersion associated with Ge is in order.

The bulk polariton dispersion relation is  $k^2 = (\omega^2/c^2)\epsilon(\omega)$ . Calculations of the dispersion curve reveal the following behavior. The results for  $\omega < 8.7\omega_g$  show that the bulk polariton wave vector is larger than the surface-polariton wave vector at a given frequency. For  $\omega \approx 5\omega_g$ , the bulk polariton curve begins to bend back, crossing the surface-polariton curve at  $\omega \approx 8.7\omega_g$ , and then remains to the left of the surface polariton curve. Calculations were made [Eq. (7)] of the ATR an-

TABLE I. Comparison of surface-polariton dispersion results and ATR calculations.

$\omega/\omega_g$	$ck/\omega_g$ [from Eq. (7)]		$ck_1/\omega_g$ [from Eq. (1)]
	(1) <sup>a</sup>	(2) <sup>b</sup>	
7.3	...	7.8	7.6
8.7	10.4	9.3	9.1
9.9	11.8	10.7	10.8
11.2	13.1	...	12.5

<sup>a</sup>Gap distance  $d=0.025 \mu\text{m}$ .

<sup>b</sup> $d=0.05 \mu\text{m}$ .

gle of incidence for bulk polaritons at various frequencies. Except for  $\omega = 8.7\omega_g$  (where the angle of incidence is  $48^\circ$ ), the differences in the incident angle for the bulk and surface polaritons are large (i. e., the differences are  $23.7$ ,  $16$ , and  $30^\circ$  for  $\omega = 7.33$ ,  $9.94$ , and  $11.18\omega_g$ . Consequently, in making ATR measurements on Ge, there should be no problem in distinguishing between bulk and surface polaritons except in the region just noted.

#### IV. DISCUSSION

The dispersion curve obtained from the experimental data (Fig. 3) shows backbending for the situation where damping is present. This type of behavior has also been observed in silver.<sup>9</sup> The backbending shows that above a certain frequency ( $\omega \approx 13.5\omega_g$ ), ordinary surface polaritons, which exist for  $k > \omega/c$ , are no longer present. Instead, we have the so-called Zenneck modes,<sup>4</sup> i. e., modes where  $k < \omega/c$ . Zenneck modes also exist in the region where  $\omega/\omega_g \lesssim 5.22$  as indicated in Fig. 4. As the frequency increases from very small values, the crossover point from Zenneck modes to ordinary surface-polariton modes which occurs at  $\omega/\omega_g \approx 5.22$  corresponds roughly to the point where  $\epsilon_1 \approx -1$  and is decreasing, as can be seen from Fig. 1. The crossover point from surface-polariton modes back to Zenneck modes occurs when  $\omega/\omega_g \approx 13.5$  and  $\epsilon_1 < -1$  and is increasing.

When damping is set to zero, several qualitative features occur. First of all, backbending is eliminated. The ordinary surface polariton which exists for  $k > \omega/c$  now approaches an asymptotic value when  $k \rightarrow \infty$  corresponding to  $\epsilon_1 = -1$ . The Zenneck modes which lie to the left of the light line,  $\omega = kc$ , now reduce to the Brewster modes<sup>13</sup> which are radiative in nature and involve only a single wave in the vacuum beyond the dielectric.

\*Work supported in part by the Office of Naval Research; a preliminary account was given at the Anaheim meeting of the American Physical Society in January, 1975 [Bull.

Am. Phys. Soc. **20**, 45 (1975)].

<sup>1</sup>J. J. Hopfield, Phys. Rev. **112**, 1555 (1958).

<sup>2</sup>A. Otto, Z. Physik. (Leipzig.) **216**, 398 (1968).

- <sup>3</sup>B. Fischer, N. Marschall, and H. J. Queisser, *Surf. Sci.* 34, 50 (1973).
- <sup>4</sup>J. Zenneck, *Ann. Phys.* 23, 846 (1907).
- <sup>5</sup>N. Marschall and B. Fischer, *Phys. Rev. Lett.* 28, 811 (1972).
- <sup>6</sup>G. Dresselhaus and M. S. Dresselhaus, *Phys. Rev.* 160, 649 (1967).
- <sup>7</sup>T. M. Donovan, E. J. Ashley, and H. E. Bennett, *J. Opt. Soc. Am.* 53, 1403 (1963).
- <sup>8</sup>L. Marton and J. Toots, *Phys. Rev.* 160, 602 (1967).
- <sup>9</sup>R. W. Alexander, G. S. Kovener, and R. J. Bell, *Phys. Rev. Lett.* 32, 154 (1974).
- <sup>10</sup>A. V. Knudsen and J. E. Kupperian, Jr., *J. Opt. Soc. Am.* 47, 440 (1947).
- <sup>11</sup>D. A. Patterson and W. H. Vaughan, *J. Opt. Soc. Am.* 53, 852 (1963).
- <sup>12</sup>M. F. Bishop, *Phys. Rev. B* 11, 901 (1975).
- <sup>13</sup>E. Burstein, A. Hartstein, J. Schoenwald, A. A. Maradudin, D. L. Mills, and R. F. Wallis, *Proceedings of the Taormina Research Conference on the Structure of Matter*, edited by E. Burstein and F. de Martini (Pergamon, Oxford, 1974), p. 89.